

## A Method to Estimate the Dynamic Displacement and Stress of a Multi-layered Pavement with Bituminous or Concrete Materials

Zheng LU<sup>1\*</sup>, Hailin YAO<sup>1</sup>, Jingbo ZHANG<sup>2</sup>

<sup>1</sup> State Key Laboratory of Geomechanics and Geotechnical Engineering, Institute of Rock and Soil Mechanics, Chinese Academy of Sciences, Xiaohongshan, Wuchang, Wuhan 430071, P. R. China

<sup>2</sup> China Second Highway Consultants Co. Ltd, No. 18, Chuangye Road, Wuhan Economic and Technologic Development Zone, Wuhan 430056, P. R. China

**crossref** <http://dx.doi.org/10.5755/j01.ms.20.4.6071>

Received 30 December 2013; accepted 04 November 2014

In this research work, a method to estimate the dynamic characteristics of a multilayered pavement with bituminous or concrete materials is proposed. A mechanical model is established to investigate the dynamic displacement and stress of the multi-layered pavement structure. Both the flexible and the rigid pavements, corresponding to bituminous materials and concrete materials, respectively, are studied. The theoretical solutions of the multi-layered pavement structure are deduced considering the compatibility condition at the interface of the structural layers. By introducing FFT (Fast Fourier Transform) algorithm, some numerical results are presented. Comparisons of the theoretical and experimental result implied that the proposed method is reasonable in predicting the stress and displacement of a multi-layered pavement with bituminous or concrete materials.

*Keywords:* inverse Fourier transform, bituminous materials, concrete materials, Young's modulus.

### 1. INTRODUCTION

With the rapid development of highway traffic, high speed and heavy vehicles increase year by year. In China, after completion for 2–3 years, a lot of pavements are damaged apparently due to high vehicle speed and overloading in the condition of road pavement unevenness. That brings some hidden troubles to safe driving, as well as leading to increasing repair workload. The higher demand for the pavement material is put forward due to the increasing vehicle load and road traffic. Extensive material destruction tests showed that the long-term performance for asphalt and concrete material are closely related to stress level [1–4]. Therefore, accurate assessment of stress level and deformation characteristics of pavement structures under traffic loading is the basis for rational design of pavement and also the key to prevent the damage of pavement material.

In fact, the pavement structure layers constructed by asphalt mixtures (flexible pavement) or concrete material (rigid pavement) often have elastic or visco-elastic properties when subjected to traffic load. Kim [5, 6] established a viscous Winkler-plate model based on the linear elastic hypothesis and the Kirchhoff thin plate theory. The influence of material properties of the plate on the displacement and stress responses were examined in their work. By incorporating the finite strip method, together with a spring system, Huang et al [7] developed a procedure to investigate the response of rectangular plate structures under moving loads. Lu et al [8] examined the effects of the dynamic vehicle-road interaction on the pavement responses by considering the visco-elastic behaviour of the foundation. However, in these studies, the

pavement-foundation system was modelled as a thin plate resting on Winkler-type foundation which was composed of spring and dashpot. Therefore, a multi-layered structure model is superior to Winkler-type models for evaluate the mechanical response of pavement systems. In order to obtain the stresses and displacements accurately, many researchers developed layered elastic or viscous elastic models for pavements [9–11]. Also, several mechanical analysis software and specifications were based on the above models [12]. These simulations treated the traffic loads as static, but the pavement structures are apparently subjected to moving dynamic loads, and the asphalt mixtures or concrete material exhibit a different behaviour from these ideal conditions. The dynamic properties of layered pavement structures should be estimated using elastodynamic approach.

The objective of present paper is therefore to estimate the dynamic displacement and stress of a multi-layered pavement with bituminous or concrete materials. Both of the dynamic characteristics of the vehicle loads and the multi-layered structural properties of the pavement are considered. The theoretical solutions are deduced according to the proposed method and the corresponding numerical results are derived. In order to validate the proposed method, the predicted displacement and stress are compared to the experimental data which are accurately measured in such a pavement structure.

### 2. THEORETICAL SOLUTIONS

A pavement structure is a multilayered system including the surface layer, base, sub-base and subgrade, on a foundation of bedrock or natural soil. Therefore, a three dimensional multilayered elastodynamic model could be used to analyze the stress and displacement due to vehicle loads. Based on the pavement structure of China, a

\*Corresponding author. Tel.: +86-27-87198350; fax: +86-27-87198350.  
E-mail address: [lzwhrsm@163.com](mailto:lzwhrsm@163.com) (Z. Lu)

3D multi-layered computing model is established, as shown in Figure 1. Supposing that the pavement materials are isotropic and homogenous, in the absence of body forces, one obtains the dynamic governing equation as following:

$$(\lambda + G)u_{j,ij} + Gu_{i,ij} = \rho \frac{\partial^2 u_i}{\partial t^2}, \quad (1)$$

where  $\lambda$  and  $G$  are Lamé parameters,  $\rho$  is the material density,  $u_i$  is the displacement vector.

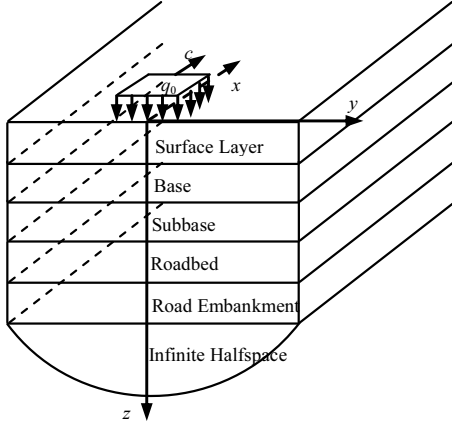


Fig. 1. 3D multi-layered pavements model

The stress-strain relation can be expressed as:

$$\sigma_{ij} = 2G\varepsilon_{ij} + \lambda e\delta_{ij}, \quad (2)$$

where  $\delta_{ij}$  is the Kronecker delta,  $e$  is the cubical dilatation of the medium,  $\sigma_{ij}$  is the component of stress tensor, and  $\varepsilon_{ij}$  is the component of strain tensor.

A double Fourier transform  $(x, y) \rightarrow (\beta, \gamma)$  and the inverse relationship can be defined as

$$\left. \begin{aligned} \bar{f}(\beta, \gamma, z) &= \int_{-\infty}^{\infty} \int_{-\infty}^{\infty} f(x, y, z) e^{-i(\beta x + \gamma y)} dx dy \\ f(x, y, z) &= \frac{1}{4\pi^2} \int_{-\infty}^{\infty} \int_{-\infty}^{\infty} \bar{f}(\beta, \gamma, z) e^{-i(\beta x + \gamma y)} d\beta d\gamma \end{aligned} \right\}, \quad (3)$$

where  $\beta, \gamma$  are the wave number in the  $x$  and  $y$  direction,  $f$  is a variable in space domain, and  $\bar{f}$  is the corresponding variable in the transformed domain.

Based on the shifting theorem of the Fourier transform given in Eq. (3), the displacements of pavement can be solved in the transformed domain. Then according to the stress-strain relation given in Eq. (2), the stresses of pavement can also be derived. All the responses of the displacements and the stresses have been given by Lu [13].

A moving rectangular load, which is assumed to be time harmonic, is applied on the road surface ( $z = 0$ ). For the rigid pavement with concrete material, a thin-plate can be employed to simulate the mechanical behavior, as in Kim [5, 6]. If the reaction of the base to the surface layer (modeled as a thin plate) is denoted as  $\varphi(x, y, t)$ , the governing equation of surface layer is given as follows:

$$\begin{aligned} D_0 \nabla^2 (\nabla^2 W) + \rho_0 h_0 \frac{\partial^2 W}{\partial t^2} + \varphi(x, y, t) &= \frac{q_0 e^{i\omega t}}{4l_1 l_2}, \\ [H(y+l_2) - H(y-l_2)] [H(x+l_1) - H(x-l_1)] \end{aligned} \quad (4)$$

in which  $H$  is the Heaviside function.  $W, h_0$  and  $\rho_0$  are the vertical displacement, thickness and density of the plate, respectively,  $q_0$  is the magnitude of the load pressure, and  $\omega$  is the excitation angular frequency,  $l_1$  and  $l_2$  are the length and width of the rectangular load, and  $D_0$  is the plate rigidity.

In this paper, the 3D pavement model consisting of several structure layers below the surface layer is used (Fig. 1). The following continuity conditions can be obtained at each interface

$$\left. \begin{aligned} \bar{\tau}_{xz} |_{z=0} &= 0; & -\Delta \bar{u}_z |_{z=0} + \bar{\sigma}_z |_{z=0} &= -Fq_0; \\ (\bar{\sigma}_z)_n &= (\bar{\sigma}_z)_{n+1}; & (\bar{u}_x)_n &= (\bar{u}_x)_{n+1}; & (\bar{\tau}_{xz})_n &= (\bar{\tau}_{xz})_{n+1}; \\ (\bar{u}_z)_n &= (\bar{u}_z)_{n+1}; & (\bar{\sigma}_x, \bar{\sigma}_y, \bar{\sigma}_z, \bar{\tau}_{xz}, \bar{u}_x, \bar{u}_y, \bar{u}_z)_{z \rightarrow \infty} &= 0 \end{aligned} \right\}, \quad (5)$$

where  $\Delta = D_0(\beta^2 + \gamma^2)^2 + \rho_0 h_0 \alpha$ ,  $F = [\sin(\beta l_1) \sin(\gamma l_2)] / \beta \gamma l_1 l_2$ .

Applying certain manipulations on Eq. (5), a relation between displacement and stress at the interface of the surface layer and base can be written as a matrix formulation:

$$[H_0][A_1 \ B_1 \ C_1 \ D_1]' = [F \ 0]', \quad (6)$$

where  $A_1, B_1, C_1$  and  $D_1$  are arbitrary constants to be determined from the boundary conditions, “ $'$ ” denotes the transpose of matrix,  $[H_0]$  is the support matrix between multi-layered road structures with details given in Eq. (7):

$$\left. \begin{aligned} H_{011} &= D_p v_{p0} + 2G_0 v_{p0}^2 + \lambda_0 \gamma_{p0}^2, & H_{012} &= -D_p v_{p0} + 2G_0 v_{p0}^2 + \lambda_0 \gamma_{p0}^2 \\ H_{013} &= -D_p (v_{s0}^2 - \gamma_{s0}^2) - 2v_{s0} (G_0 v_{s0}^2 - \rho_0 \alpha), & H_{014} &= -D_p (v_{s0}^2 - \gamma_{s0}^2) + 2v_{s0} (G_0 v_{s0}^2 - \rho_0 \alpha) \\ H_{021} &= -2iG_0 \beta \gamma v_{p0}, & H_{022} &= 2iG_0 \beta \gamma v_{p0}, & H_{023} &= i\beta (2G_0 v_{s0}^2 - \rho_0 \alpha), & H_{024} &= i\beta (2G_0 v_{s0}^2 - \rho_0 \alpha) \end{aligned} \right\}, \quad (7)$$

where  $v_p^2 = \beta^2 + \gamma^2 - (\omega - \beta c)^2 / c_p^2$ ;  $v_s^2 = \beta^2 + \gamma^2 - (\omega - \beta c)^2 / c_s^2$ .  $c_p$  and  $c_s$  are the compression (P-waves) and shear wave (S-waves) speed of elastic medium, respectively. The subscript “0” denotes the parameters for the first layer. More details are presented in reference [13].

Similarly, at the interface of  $z_n$ , the following matrix formulation can be obtained:

$$[A_n \ B_n \ C_n \ D_n]' = [M_n][A_{n+1} \ B_{n+1} \ C_{n+1} \ D_{n+1}]' \quad (8)$$

where the subscript “ $n$ ” denotes the parameters for the  $n$ th layer,  $[M_n] = [H_n]^{-1} |_{z=z_n} [H_{n+1}] |_{z=z_n}$ , in which  $[H_n]$  is transfer matrix of the road structure layers, its dimensions are  $4 \times 4$  and is detailed in Eq. (9):

$$\left. \begin{aligned} H_{n11} &= e^{-v_{pn} z}, & H_{n12} &= e^{v_{pn} z}, & H_{n13} &= -v_{sn} e^{-v_{sn} z}, & H_{n14} &= v_{sn} e^{v_{sn} z}, & H_{n21} &= -v_{pn} e^{-v_{pn} z}, & H_{n22} &= v_{pn} e^{v_{pn} z} \\ H_{n23} &= (v_{sn}^2 - \gamma_{sn}^2) e^{-v_{sn} z}, & H_{n24} &= (v_{sn}^2 - \gamma_{sn}^2) e^{v_{sn} z}, & H_{n31} &= (2G_n v_{pn}^2 + \lambda_n \gamma_{pn}^2) e^{-v_{pn} z}, \\ H_{n32} &= (2G_n v_{pn}^2 + \lambda_n \gamma_{pn}^2) e^{v_{pn} z}, & H_{n33} &= -2v_{sn} (G_n v_{sn}^2 - \rho_n \alpha) e^{-v_{sn} z}, & H_{n34} &= 2v_{sn} (G_n v_{sn}^2 - \rho_n \alpha) e^{v_{sn} z}, \\ H_{n41} &= -2G_n v_{pn} e^{-v_{pn} z}, & H_{n42} &= 2G_n v_{pn} e^{v_{pn} z}, & H_{n43} &= (2G_n v_{sn}^2 - \rho_n \alpha) e^{-v_{sn} z}, & H_{n44} &= (2G_n v_{sn}^2 - \rho_n \alpha) e^{v_{sn} z} \end{aligned} \right\}. \quad (9)$$

If the last layer of road structures is half-space, there are no propagating waves in the negative  $z$  direction (no reflection), so we get

$$B_N = D_N = 0. \quad (10)$$

Applying certain manipulations on Eqs. (6) and (8), we have

$$[F \ 0]' = [M][A_N \ 0 \ C_N \ 0]', \quad (11)$$

where  $[M] = [H_0] \left( \prod_{n=1}^{N-1} [M_n] \right)$ .

If the road structure is built on rigid bedrock, namely the thickness of bottom layer is infinite, the displacements at the bottom of the  $N^{\text{th}}$  layer can be treated as zero. Therefore, we can obtain that

$$[Q][A_N \ B_N \ C_N \ D_N]' = [0 \ 0]', \quad (12)$$

where  $[Q]$  is the support matrix between rigid bedrock and multi-layered structures and it is detailed in Eq. (13):

$$\left. \begin{aligned} Q_{11} &= e^{-\nu_{pN} z_N}, Q_{12} = e^{\nu_{pN} z_N}, Q_{13} = -\nu_{sN} e^{-\nu_{sN} z_N}, Q_{14} = \nu_{sN} e^{\nu_{sN} z_N}, Q_{21} = -\nu_{pN} e^{-\nu_{pN} z_N} \\ Q_{22} &= \nu_{pN} e^{\nu_{pN} z_N}, Q_{23} = (\nu_{sN}^2 - \gamma_{sN}^2) e^{-\nu_{sN} z_N}, Q_{24} = (\nu_{sN}^2 - \gamma_{sN}^2) e^{\nu_{sN} z_N} \end{aligned} \right\}. \quad (13)$$

From Eqs. (6), (8) and (12), the following expression can be derived:

$$[M \ Q][A_N \ B_N \ C_N \ D_N]' = [F \ 0 \ 0 \ 0]'. \quad (14)$$

According to Eqs. (10) and (11) or (14), four constants  $A_N, B_N, C_N$  and  $D_N$  can be obtained. After determining the constants in the bottom layer, one can obtain all the constants from the bottom layer to the top layer. By applying the double inverse Fourier transform given in Eq. (3), the displacements and the stresses in the time domain can be expressed uniformly as follows:

$$\Pi(x, y, z, t) = \frac{1}{4\pi^2} \int_{-\infty}^{\infty} \int_{-\infty}^{\infty} \bar{\Pi}(\beta, \gamma, z) e^{-i[\beta(x-ct)+\gamma y]} e^{i\alpha t} d\beta d\gamma, \quad (15)$$

where

$\bar{\Pi}(\beta, \gamma, z) = (\bar{u}_x, \bar{u}_y, \bar{u}_z, \bar{\sigma}_x, \bar{\sigma}_y, \bar{\sigma}_z, \bar{\tau}_{xz}, \bar{\tau}_{yz}, \bar{\tau}_{xy})(\beta, \gamma, z)$  are the components of displacement tensors and stress tensors given by Lu [13]. For the situation of the flexible pavement, the corresponding solutions can be easily derived by reducing the thickness of the thin plate to zero.

### 3. VERIFICATION OF DYNAMIC VERTICAL STRESS

The components of dynamic response derived above are very important in predicting the mechanical behavior of pavement structures. Thus it is necessary to verify the theoretical solutions with experimental measurements. A multilayered pavement model is built based on the laboratory model tests performed by Lu [14]. All the calculation parameters of pavement materials in this paper are shown in Table 1, which are the same as those derived by Lu [14].

**Table 1.** Material properties of pavement structure layers

| Pavement structure layers | Young's modulus, MPa | Thickness, m | Density, kg/m <sup>3</sup> | Poisson ratio |
|---------------------------|----------------------|--------------|----------------------------|---------------|
| Surface layer             | 1400                 | 0.18         | 2400                       | 0.30          |
| Base                      | 735                  | 0.30         | 2230                       | 0.30          |
| Subbase                   | 637                  | 0.30         | 2195                       | 0.30          |
| Subgrade layer 1          | 45                   | 0.30         | 1981                       | 0.35          |
| Subgrade layer 2          | 29                   | 0.30         | 1992                       | 0.35          |
| Subgrade layer 3          | 37                   | 0.45         | 1955                       | 0.35          |

According to the laboratory physical model, the double-circular loads are used to simulate the vehicle loads. However, the shape of the contact area between

vehicle tires and pavement has been proved to be square [15]. Therefore, the double-rectangular loads is superior to the double-circular ones for evaluate the tire-pavement pressure. In this section, the double-rectangular loads are adopted and the pressure of each tire is the same as the experimental loading. Afterwards, the dynamic solutions derived in Section 2.1 could be employed for the calculations.

A semi-sinusoidal wave is adopted to simulate the moving traffic loads in the laboratory model tests, and the numerical results are obtained by solving Eq. (15) through the inverse fast Fourier transform method. The calculation points are the same as the measuring points shown in Lu [14]. Fig. 2 compares the vertical stress obtained from experimental measurements with that from theoretical calculations.

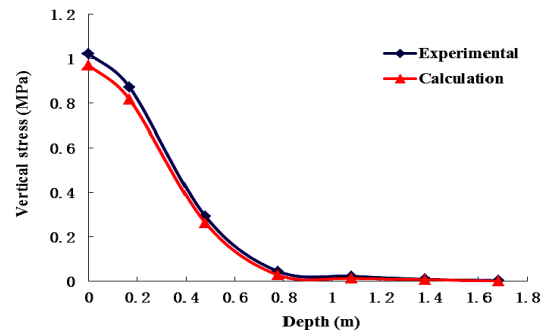


**Fig. 2.** Comparison between present results and experimental ones

From Fig. 2, we can see that the values of the vertical stress from calculation are of little difference from those of experimental ones in the range of  $z \geq 0.5$  m. But in the initial range of  $z$  ( $0 \text{ m} \leq z \leq 0.5 \text{ m}$ ), the values of the vertical stress from calculation are smaller than those of experimental ones. It might be due to the fact that the applied loads in the calculation are double-rectangular type rather than the double-circular type in the experiments. In the vicinity of load area ( $0 \text{ m} \leq z \leq 0.5 \text{ m}$ ), the difference between the theoretical calculations and experimental data might be explained by Saint-Venant principle. However, the total trend of numerical results derived by present method and the experimental ones agree well with each other.

### 4. EFFECTS OF MATERIAL PROPERTIES OF PAVEMENT ON THE RESPONSES

The dynamic response analysis of pavement plays an important role in the design and maintenance of pavement. The variations of stresses and displacements of a pavement structure are depends heavily on its material properties. Therefore, the effects of material properties of pavement on the dynamic stresses and displacements should be further investigated. As we know, a structure layer of pavement is often composed of aggregates. According to the theory of elastic dynamics, two elastic parameters (the Young's modulus and Poisson's ratio) can be employed to characterize the properties of such material. In this section, the variations of dynamic stresses and displacements with different pavement Young's modulus are analyzed to

illustrate the effects of material properties on its mechanic responses.

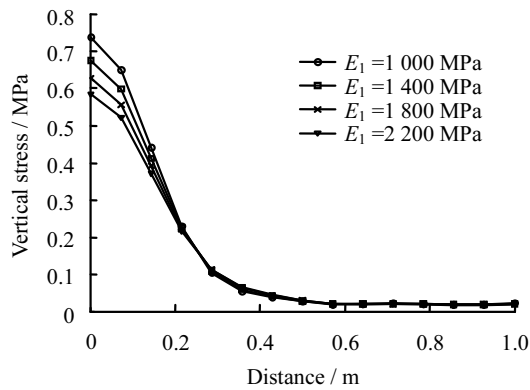


Fig. 3. Distribution of the vertical stress along the longitudinal direction

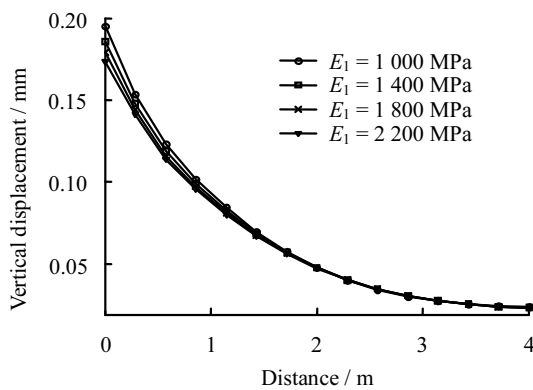


Fig. 4. Distribution of the vertical displacement along the longitudinal direction

In Figs. 3 and 4, a flexible pavement is chosen for numerical example, and the Young's modulus is calculated from 1000 MPa to 2200 MPa, which represents the most general situations of a flexible pavement made of bituminous materials. From Fig. 3, we can see that the curves of different pavement Young's modulus have the similar changes. The vertical stress decreases significantly near the loading area and the curves gradually flatten when far away from the load center. The vertical stress of pavement decreases clearly with the increasing of the pavement Young's modulus. Obvious differences of the curves, which reflect the influence of different pavement Young's modulus, can be observed only near the region of loading area. The vertical displacement distributions corresponding to different pavement modulus are calculated and shown in Fig. 4. As can be seen, the vertical displacement of pavement decreases with the increasing of the pavement Young's modulus, which follows the similar rules accordingly as that in Fig. 3. Through comparison of Fig. 3 and Fig. 4, we find that the attenuation of the vertical stress, as far as the transverse direction is concerned, is visibly faster than those of the vertical displacement.

## 5. CONCLUSIONS

In this paper, a method has been presented to estimate the dynamic displacement and stress of a multi-layered

pavement made of bituminous or concrete materials. Both the flexible pavements and the rigid pavements, which are corresponding to bituminous materials and concrete materials, respectively, have been studied. The main conclusions of this study can be summarized as follows:

1. A multi-layered pavement model is built and the flexible pavement is considered as a multilayered structure with homogenous, isotropic elastic medium, and the rigid pavement is also regarded as a thin-plate resting on a multilayered structure.

2. The dynamic equilibrium equations of the pavements are solved on the basis of assembly process compatible with good numerical efficiency, and results from the calculations are verified using model experiment data.

3. The vertical responses decrease significantly near the loading area and the curves gradually flatten when far away from the load center. Obvious differences of the curves, which reflect the influence of different pavement Young's modulus, can be observed only near the region of loading area.

4. The analysis also showed that the attenuation of the vertical stress, as far as the transverse direction is concerned, is visibly faster than those of the vertical displacement.

## Acknowledgement

This research is supported by the National 973 Project of China (No. 2013CB036405) and the Natural Science Foundation of China (No. 41472286 and 51209201). The constructive comments from the anonymous referees are highly acknowledged.

## REFERENCES

1. **Setyawan, A.** Assessing The Compressive Strength Properties of Semi-Flexible Pavements *Procedia Engineering* 54 2013: pp. 863–874.
2. **Mensching, D. J., McCarthy, L.-M., Mehta, Y.** Modeling Flexible Pavement Overlay Performance For Use With Quality-Related Specifications *Construction and Building Materials* 48 2013: pp. 1072–1080. <http://dx.doi.org/10.1016/j.conbuildmat.2013.07.058>
3. **Pozarycki, A., Garbowski, T.** Laboratory Testing of Fatigue Crack Growth in Geosynthetically Reinforced Large Scale Asphalt Pavement Samples *Procedia Engineering* 57 2013: pp. 922–928.
4. **Xue, Q., Liu, L.** Hydraulic-stress Coupling Effects on Dynamic Behavior of Asphalt Pavement Structure Material *Construction and Building Materials* 43 2013: pp. 31–36.
5. **Kim, S.-M.** Influence of Horizontal Resistance at Plate Bottom on Vibration of Plates on Elastic Foundation under Moving Loads *Engineering Structures* 26 (2) 2004: pp. 519–529. <http://dx.doi.org/10.1016/j.engstruct.2003.12.002>
6. **Kim, S.-M.** Buckling and Vibration of a Plate on Elastic Foundation Subjected to In-plane Compression and Moving Loads *International Journal of Solids and Structures* 41 2004: pp. 5647–5661.
7. **Huang, M.-H., Thambiratnam, D.-P.** Deflection Response of Plate on Winkler Foundation to Moving Accelerated

- Loads *Engineering Structures* 23 (6) 2001: pp. 1134–1141.
8. **Lu, Z., Yao, H.-L.** Effects of the Dynamic Vehicle-road Interaction on the Pavement Vibration due to Road Traffic *Journal of Vibroengineering* 15 (3) 2013: pp.1291–1301.
  9. **Gajewski, J., Sadowski, T.** Sensitivity Analysis of Crack Propagation in Pavement Bituminous Layered Structures Using a Hybrid System Integrating Artificial Neural Networks and Finite Element Method *Computational Materials Science* 82 (1) 2014: pp.114–117.
  10. **Xue, Q., Liu, L., Ying, Z.** Dynamic Behavior of Asphalt Pavement Structure under Temperature-stress Coupled Loading *Applied Thermal Engineering* 53 2013: pp.1–7. <http://dx.doi.org/10.1016/j.applthermaleng.2012.10.055>
  11. **Eyal, L.** Analysis of Pavement Response to Subsurface Deformations *Computers and Geotechnics* 50 (5) 2013: pp. 79–88.
  12. Specifications for Design Highway Asphalt Pavement (JTGD50–2006), Beijing: China Communications Press, 2006.
  13. **Lu, Z., Yao, H.-L., Luo, X.-W., Hu, M.-L.** 3D Dynamic Responses of Layered Ground under Vehicle Loads *Rock and Soil Mechanics* 30 (10) 2009: pp. 2965–2970.
  14. **Lu, Z., Yao, H.-L., Liu, J.** Laboratory Model Experiments on Dynamic Behavior of Road Structures under Repeated Traffic Loads *Modelling and Computation in Engineering* 11 2011: pp. 33–38.
  15. **James, W.-M., Yoshiaki, O., Kunihito, M.** Linear Elastic Analysis of Pavement Structure under Non-circular Loading *Road Materials and Pavement Design* 13 (3) 2012: pp. 403–421.